

Research Letter

Influence of doped metal center on morphology and pore structure of ZIF-8

Ahmed Awadallah-F*, Department of Chemical Engineering, Qatar University, P.O. Box 2713, Doha, Qatar Febrian Hillman, Artie McFerrin Department of Chemical Engineering, Texas A&M University, College Station, USA Shaheen A. Al-Muhtaseb , Department of Chemical Engineering, Qatar University, P.O. Box 2713, Doha, Qatar Hae-Kwon Jeong, Artie McFerrin Department of Chemical Engineering, Texas A&M University, College Station, USA; Department of Materials Science and Engineering, Texas A&M University, College Station, TX 77843-3122, USA

Address all correspondence to Shaheen A. Al-Muhtaseb at s.almuhtaseb@qu.edu.qa

(Received 23 September 2018; accepted 29 October 2018)

Abstract

Synthesis of ZIF with zinc, cobalt, or copper was carried out by microwaves. The effect of metal center on morphologies and pores of products was studied. Nitrogen adsorption/desorption onto ZIFs was examined by density functional theory. The micro, meso, and macropores of ZIF-8, Zn/Co-ZIF-8, and Cu/ZIF-8 ranged 99.814–99.969%, 0.055–0%, and 0.031–0.130%, respectively. Average pore sizes of ZIF-8, Zn/Co-ZIF-8, and Cu/ZIF-8 are 1.291, 1.194, and 1.164 nm, respectively. Monolayer saturation limits of nitrogen onto ZIF-8, Zn/Co-ZIF-8, and Cu/ZIF-8 were 21.152, 18.943, and 17.784 mmol/g, respectively. Further, the results included densities, total surface areas, total pore volumes, and average particle sizes of ZIF-8, Zn/Co-ZIF-8, and Cu/ZIF-8.

Introduction

Zeolitic imidazolate frameworks (ZIFs) are porous crystalline materials consisting of well-ordered pores.^[1] These materials are consisting of metal cluster nodes and organic linkers. [2,3] They have high-surface areas and adsorption capacities; and often exhibit high thermal, chemical, and hydrothermal stabilities. [4] Their intrinsic porous characteristics, abundant functionalities as well as their exceptional thermal and chemical stabilities render ZIFs attractive candidates for a wide range of applications such as gas storage, molecular separation, catalysis, drug delivery, and chemical sensors. [5–7] Properties, types, and structures of ZIFs depend mainly on different combinations of imidazole linkers and metal ions. [8,9] The literature reports a great number of ZIFs, which can be synthesized by different transition metals, imidazole linkers, and solvents such as water, dimethylformamide, diethylformamide, ethanol, and methanol.[10,11] ZIFs can be synthesized by solvothermal or hydrothermal synthesis methods at temperatures between 25 and 150 °C using an excess amount of imidazole. [12] Cu(II) and Zn(II) metal-organic framework films on metal substrates were prepared by various techniques such as sonochemical technique.[13]

The object of this communication letter is to study the effect of metal center type on morphology and pore structure of ZIF-8 analogs. Metal centers used are Co²⁺ and Cu²⁺. Morphology

investigation will be measured by NanoSEM and transmission electron microscopy (TEM). Nitrogen gas adsorption/desorption at 77 K into ZIF-8 products will be investigated. Pore structure will be studied by density functional theory (DFT). Pore structures include total surface areas in pores wider than 0.5 nm, total pore volume, average particle sizes, DFT total surface area energy, average pore size, and percentages of micropores, mesopores, and macropores.

Experimental

Zn(NO₃)₂·6H₂O (98%, Sigma Aldrich) and Cu(NO₃)₂·2.5H₂O (≥99.99%, Sigma Aldrich), and Co(NO₃)₂·6H₂O (98%, Sigma Aldrich) were used as metal centers. 2-Methylimidazole (C₄H₅N₂, 97%, Sigma Aldrich) was used as a linker. Nitrogen and helium (99.999%) were purchased from NIGP (Doha, Qatar). Methanol (99.8%, Alfa Aesar) was used as solvent. Other chemicals were used without further purification. Full details of synthesis of ZIF-8, Zn/Co-ZIF-8 and Cu/ZIF-8 and their characterizations are found in Supplementary data.

Results and discussion

Figures 1(a)–1(f) show NanoSEM and TEM photomicrographs of ZIF-8, Zn/Co-ZIF-8, and Cu/ZIF-8. It was observed that the presence of copper and cobalt metal centers in the matrix of ZIF-8 leads to changing morphologies in both surface and bulk. Photomicrographs of Figs. 1(a), 1(c), and 1(e) refer to images by NanoSEM, whereas Figs. 1(b), 1(d), and 1(f) refer to TEM. It can be noted from Fig. 1(c) that particle sizes of Zn/Co-ZIF-8 is larger than those of ZIF-8 and Cu/ZIF-8

^{*} On leave from the Radiation Research of Polymer Department, National Centre for Radiation Research and Technology, Atomic Energy Authority, P.O. Box 29, Nasr City, Cairo, Egypt.

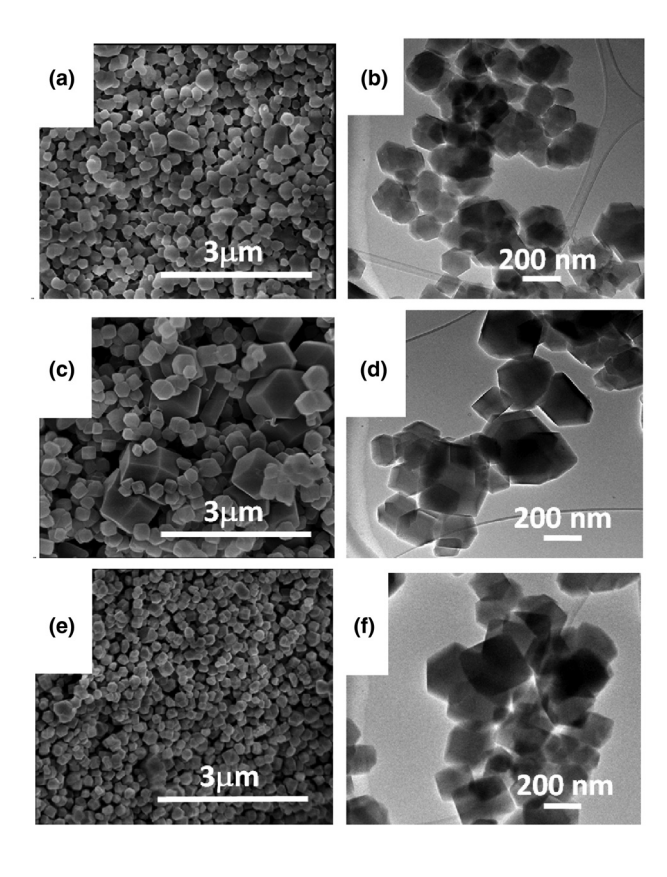


Figure 1. NanoSEM (a, c and e) and TEM (b, d and f) photomicrographs of ZIF-8 (a and b), Zn/Co-ZIF-8 (c and d), and Cu/ZIF-8 (e and f). Scale bar lengths in NanoSEM is 3 μm , and in TEM 200 nm.

presented in Figs. 1(a) and 1(e), respectively. Therefore, it is clear that metal center type affects morphology of ZIFs. TEM photomicrographs presented in Figs. 1(b), 1(d), and 1(f) refer to ZIF-8, Zn/Co-ZIF-8, and Cu/ZIF-8, respectively. TEM images show transparent crystals, where even the edge line of the TEM grid behind some crystals is exposed. Further, crystals in the background could also be seen. This indicates that samples are somewhat transparent to electrons.

Figure 2(a) shows adsorption/desorption of N₂ at 77 K on samples. Maximum amounts of N₂ adsorbed onto ZIF-8, Zn/ Co-ZIF-8, and Cu/ZIF-8 are 18.327, 18.858, and 17.784 mmol/g, respectively. Zn/Co-ZIF-8 exhibits the highest capacity, whereas Cu/ZIF-8 exhibits the lowest capacity. Therefore, metal center type has a noticeable effect on amount of N₂. Further, it was observed that there is a very small hysteresis loop [in sub-Fig. 2(b)] during adsorption/desorption at P/P_0 > 0.95 (P is the pressure and P_0 is saturation pressure of N_2 at 77 K [0.954 atm]). Consequently, there is small capillary condensation occurring during adsorption/desorption at a highrelative pressures. Typical type-I isotherms were obtained for samples, which declares the presence of almost full microporosity. [14] However, behavior of isotherms for P/P_0 values beyond 0.95 changes to type-IV, which may refer to the existence of very small amount of large pores due to intra-aggregate

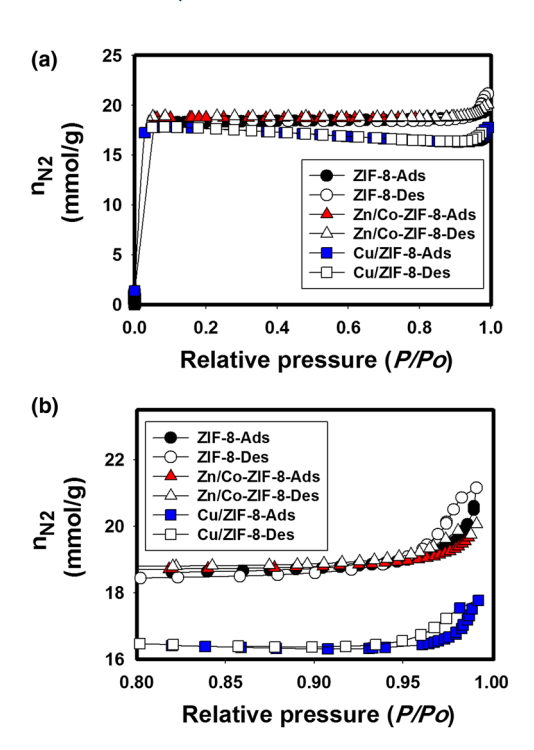


Figure 2. (a) Adsorption/desorption of N₂ onto ZIF-8, Zn/Co-ZIF-8, and Cu/ ZIF-8 and (b) subfigure of adsorption/desorption of N2 onto ZIF-8, Zn/ Co-ZIF-8, and Cu/ZIF-8 at 77 K.

voids.[15] Results of adsorption/desorption agreed with DFT data listed in Table I.

Figures 3(a) and 3(b) show the effect of pore width on cumulative and incremental surface areas of ZIF-8, Zn/ Co-ZIF-8, and Cu/ZIF-8. Figure 3(a) illustrates the relationship between pore size and cumulative area. It was noticed that Zn/ Co-ZIF-8 exposes the highest cumulative area and Cu/ZIF-8 represents the lowest one. Sequential order of cumulative area is Zn/Co-ZIF-8 > ZIF-8 > Cu/ZIF-8, and their corresponding cumulative areas are 987.2, 963.0, and 972.8 m²/g, respectively. Furthermore, the relationship between pore width and cumulative area is constant after ~2 nm, which indicates that no micropores existed beyond that value. Values of area, average pore width, and other parameters related to pore structure are listed in Table I. Figure 3(b) illustrates the influence of pore width on incremental area. It was seen that incremental area increased only at specific range of pore width value (between 1.0 and 1.34 nm). Incremental area increased significantly with a maximum value at 1.1 nm (x-axis with log scale and truncated from >1.7 nm to show the change), which indicates that this is the most frequent micropore width in samples. The corresponding maximum incremental area values are 546.0, 902.1, and 484.9 m²/g for ZIF-8, Zn/Co-ZIF-8, and Cu/ZIF-8, respectively.

Figures 4(a) and 4(b) show distributions of cumulative and incremental pore volumes of ZIF-8, Zn/Co-ZIF-8, and Cu/ ZIF-8 with pore width. It was observed from Fig. 4(a) that



Table I. Characteristics of ZIF-8, Zn/Co-ZIF-8, and Cu/ZIF-8.

Sample	Conc. (wt%)	Total area in pores ≥ 0.5 nm (m ² /g)	Total volume (cm³/g)	n _{N2} (mmol/g)	Average particle size (nm) ^a	DFT surface energy; total area (m²/g) ^a	Micropores (%) ^b	Mesopores (%) ^b	Macropores (%)	Average pore width (nm)	Skeleton density (g/cm³) ^c
ZIF-8	Zn = 1.04	963.0	0.621 at pore ≤147.6 nm	18.327	98.3	~1729	99.814	0.055	0.130	1.291	0.290
Zn/Co-ZIF-8	Zn/Co-ZIF-8 Zn = 0.39 Co = 0.29	987.2	0.576 at pore ≤147.6 nm	18.858	102.6	~1749	99.942	0	0.053	1.194	0.319
Cu/ZIF-8	2n = 0.77 Cu = 0.10	872.8	0.511 at pore ≤172.1 nm	17.784	126.0	~126	696.66	0	0.031	1.164	0.135

^oCalculated from reported proportions of cumulative areas pores, micropores <2, mesopores >2 to 50 nm, and balance is macropores. Obtained from built-in calculations in Micromeritics ASAP2420 (DFT model).

^[16] Calculated from the ratio of mass to volume as obtained from buoyancy measurements in helium.

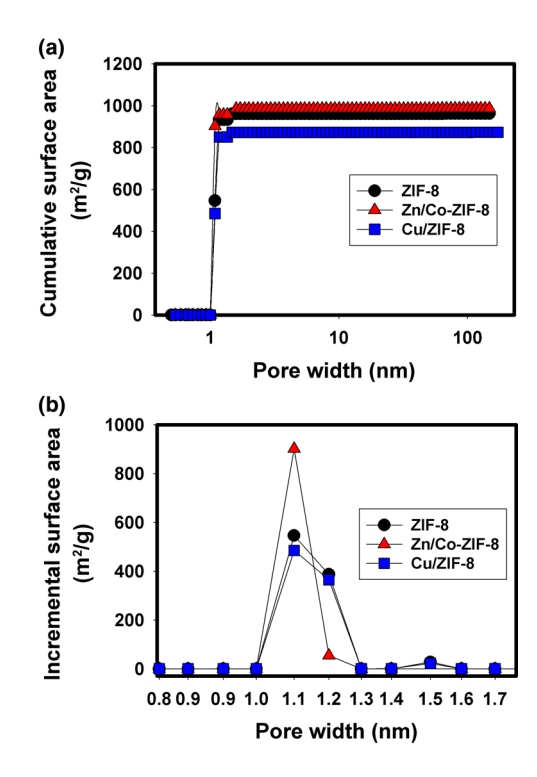


Figure 3. Relationships between the pore width and (a) cumulative area, and (b) incremental area of ZIFs.

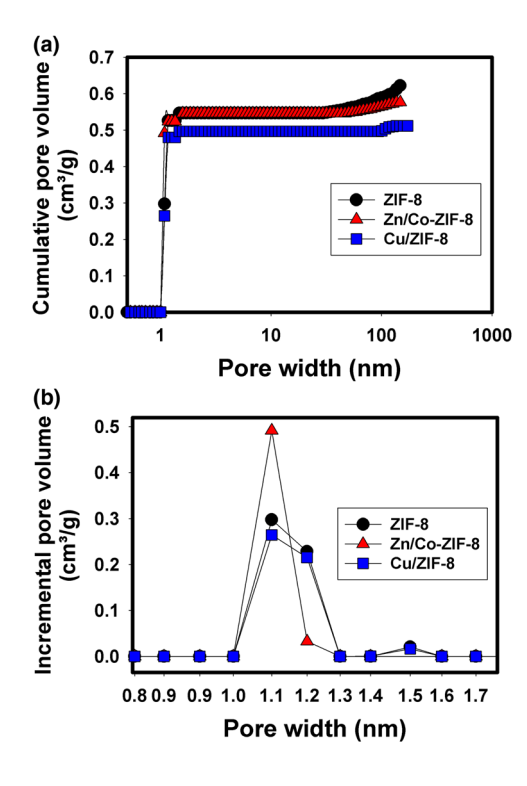


Figure 4. Relationship between the pore width and (a) cumulative volume and (b) incremental volume of ZIFs.

the effect of pore width on cumulative volume has a significant increment at 1.088 nm for Zn/Co-ZIF-8 and 1.126 nm for both of ZIF-8 and Cu/ZIF-8. Effect of pore width on cumulative volume >1.233 nm for Zn/Co-ZIF-8 and >1.306 nm for both of ZIF-8 and Cu/ZIF-8 are non-significant. It was noticed that the cumulative volume of ZIF-8, Zn/Co-ZIF-8, and Cu/ZIF-8 are 0.621, 0.576, and 0.511 cm³/g, respectively. Cumulative volume of Zn/Co-ZIF-8 is the highest whereas that of Cu/ ZIF-8 is the lowest. Figure 4(b) shows the influence of pore width on incremental volumes of ZIF-8, Zn/Co-ZIF-8, and Cu/ZIF-8. It is clear that pore width has effect only at a specific range on incremental volume (between ~ 1.0 and ~ 1.3 nm) and a non-significant effect on rest of range. Furthermore, maximum incremental volume value was 0.491 cm³/g for Zn/ Co-ZIF-8 at a pore width of 1.1 nm. On the other hand, maximum values of incremental volumes of ZIF-8 and Cu/ZIF-8 are, respectively, 0.316 and 0.228 cm³/g at 1.2 nm. Therefore, it could be said that metal center type has a significant effect on both cumulative and incremental volume. The deduced pore properties from the Micromeritics ASAP-2420® surface area analyzer for ZIF-8, Zn/Co-ZIF-8, and Cu/ZIF-8 are listed in TABLE I. Moreover, the comparison of this work with other approaches was found in Table S1 (Supplementary Data).

Conclusions

This study tackled influence of metal center type on morphology and pore structure of ZIF-8 analogs as ZIF-8, Co/ZIF-8, and Cu/ZIF-8. Pore properties were investigated by DFT of nitrogen adsorption/desorption. Amount of N2 adsorbed, incremental and cumulative area, incremental and cumulative volume, and DFT total areas, average pore width, average particle size, DFT total surface energy, and pore structure distributions were studied. Results showed that samples constitute from almost microporous structure and their average pore widths ranged from 1.64 to 1.291 nm. Morphology was analyzed by NanoSEM and TEM. Results showed that samples constitute from crystals with different sizes depending on metal type. Overall, results indicate that metal type has a significant impact on ZIF-8 morphology and pore structure as well.

Supplementary material

The supplementary material for this article can be found at https://doi.org/10.1557/mrc.2018.221.

Acknowledgments

This publication was made possible by NPRP awards (NPRP 08-014-2-003 and NPRP-8-001-2-001) from Qatar National Research Fund (a member of Qatar Foundation). H.K.-J. acknowledges support from National Science Foundation (CMMI-1561897). Statements made herein are solely the responsibility of authors. Technical support from the Department of Chemical Engineering and Central Laboratory Unit (CLU) at Qatar University is also acknowledged.

References

- 1. M. Gomar and S. Yeganegi: Adsorption of 5-fluorouracil, hydroxyurea and mercaptopurine drugs on zeolitic imidazolate frameworks (ZIF-7, ZIF-8 and ZIF-9). Microporous Mesoporous Mater. 252, 167-172 (2017).
- K. Biradha, A. Ramanan, and J.J. Vittal: Coordination polymers versus metal – organic frameworks. Cryst. Growth Des. 9, 2969–2970 (2009).
- S. Kitagawa, K. Kitaura, and S. Noro: Functional porous coordination polymers. Angew. Chem. Int. Ed. 43, 2334-2375 (2004).
- 4. K.S. Park, Z. Ni, A.P. Côté, Y.J. Choi, R. Huang, F.J. Uribe-Romo, H. K. Chae, M. O'Keeffe, and M.O. Yaghi: Exceptional chemical and thermal stability of zeolitic imidazolate frameworks. Proc. Natl. Acad. Sci. 103, 10186-10191 (2006).
- 5. R. Banerjee, A. Phan, B. Wang, C. Knobler, H. Furukawa, M. O'Keeffe, and O.M. Yaghi: High-throughput synthesis of zeolitic imidazolate frameworks and application to CO₂ capture. Science 319, 939-943 (2008).
- H. Bux, F. Liang, Y. Li, J. Cravillon, M. Wiebcke, and J. Caro: Zeolitic imidazolate framework membrane with molecular sieving properties by microwave-assisted solvothermal synthesis. J. Am. Chem. Soc. 131, 16000-16001 (2009).
- 7. Y. Pan and Z. Lai: Sharp separation of C2/C3 hydrocarbon mixtures by zeolitic imidazolate framework-8 (ZIF-8) membranes synthesized in aqueous solutions. Chem. Commun. 47, 10275-10277 (2011).
- 8. B. Chen, Z. Yang, Y. Zhu, and Y. Xia: Zeolitic imidazolate framework materials: recent progress in synthesis and applications. J. Mater. Chem. A2, 16811-16831 (2014).
- 9. X. Wang, J. Liu, S. Leong, X. Lin, J. Wei, B. Kong, Y. Xu, Z.-X. Low, J. Yao, and H. Wang: Rapid construction of ZnO@ZIF-8 heterostructures with size-selective photocatalysis properties. ACS Appl. Mater. Interfaces 8, 9080-9087 (2016).
- 10. F. Sahin, B. Topuz, and H. Kalıpçılar: Synthesis of ZIF-7, ZIF-8, ZIF-67 and ZIF-L from recycled mother liquors. Microporous Mesoporous Mater. 261, 259-267 (2018).
- 11. Y. Li, K. Zhou, M. He, and J. Yao: Synthesis of ZIF-8 and ZIF-67 using mixed-base and their dye adsorption. Microporous Mesoporous Mater. 234, 287-292 (2016).
- 12. S. Bhattacharjee, M.S.M. Jang, H.J. Kwon, and W.S. Ahn: Zeolitic imidazolate frameworks: synthesis, functionalization, and catalytic/adsorption applications. Catal. Surv. Asia 18, 101-127 (2014).
- 13. O. Abuzalat, D. Wong, M. Elsayed, S. Park, and S.W. Kim: Sonochemical fabrication of Cu(II) and Zn(II) metal-organic framework films on metal substrates. Ultrason. Sonochem. 45, 180-188 (2018).
- 14. K.S.W. Sing, D.H. Everett, R.A.W. Haul, L. Moscou, R.A. Pierotti, J. Rouquerol, and T. Siemieniewska: Reporting physisorption data for gas/solid systems with special reference to the determination of surface area and porosity. Pure Appl. Chem. 57, 603-619 (1985).
- 15. J. dos Santos, F. da Silva, D.L. Mal, G.A. Bataglion, M.N. Eberlin, C. M. Ronconi, S.A. Júnior, and G.F. de Sá: Adsorption in a fixed-bed column and stability of the antibiotic oxytetracycline supported on Zn (II)-[2-methylimidazolate] frameworks in aqueous media. PLoS ONE 10, e0128436 (2015).
- 16. A. Awadallah-F and S.A. Al-Muhtaseb: Carbon dioxide sequestration and methane removal from exhaust gases using resorcinol-formaldehyde activated carbon xerogel. Adsorption 19, 967-977 (2013).